Warming of the World Ocean

Sydney Levitus,* John I. Antonov, Timothy P. Boyer, Cathy Stephens

We quantify the interannual-to-decadal variability of the heat content (mean temperature) of the world ocean from the surface through 3000-meter depth for the period 1948 to 1998. The heat content of the world ocean increased by $\sim 2 \times 10^{23}$ joules between the mid-1950s and mid-1990s, representing a volume mean warming of 0.06°C. This corresponds to a warming rate of 0.3 watt per meter squared (per unit area of Earth's surface). Substantial changes in heat content occurred in the 300- to 1000-meter layers of each ocean and in depths greater than 1000 meters of the North Atlantic. The global volume mean temperature increase for the 0- to 300-meter layer was 0.31°C, corresponding to an increase in heat content for this layer of $\sim 10^{23}$ joules between the mid-1950s and mid-1990s. The Atlantic and Pacific Oceans have undergone a net warming since the 1950s and the Indian Ocean has warmed since the mid-1960s, although the warming is not monotonic.

The Intergovernmental Program on Climate Change (*1*), the World Climate Research Program CLIVAR (*2*), and the U.S. National Research Council (*3*) have identified the role of the ocean as being critical to understanding the variability of Earth's climate system. Physically we expect this to be so because of the high density and specific heat of seawater. Water can store and transport large amounts of heat.

Simpson (*4*) conducted the first study of Earth's heat balance which concluded that the Earth system is not in local radiative balance, and therefore transport of heat from the tropics to the poles is required for the Earth system to be in global radiative balance. Identifying the mechanisms by which heat is transported from the tropics to the poles is one of the central problems of climate research. In addition, Rossby (*5*) drew attention to the fact that because of its large specific heat capacity and mass, the world ocean could store large amounts of heat and remove this heat from direct contact with the atmosphere for long periods of time. The results of these studies are the subject of this research article.

Until recently, little work has been done in systematically identifying ocean subsurface temperature variability on basin and global scales, in large part due to the lack of data [recent studies include (*6–8*)]. The first step in examining the role of the ocean in climate change is to construct the appropriate databases and analysis fields that can be used to describe ocean variability. About 25 years ago, ship-of-opportunity programs were initiated to provide measurements of subsurface upper ocean temperature. Before the initiation of these programs, subsurface oceanographic data were not reported in real time, as is the case with much meteorological data. During the past 10 years, projects have been initiated (*9*) that have resulted in a large increase in the amount of historical upper ocean thermal data available to examine the interannual variability of the upper ocean. Using these data, yearly, objectively analyzed, gridded analyses of the existing data were prepared and distributed (*7*) for individual years for the period 1960 to 1990. We have used the recently published *World Ocean Database 1998* (*10–13*) to prepare yearly and year-season objectively analyzed temperature anomaly fields. Detailed information about the temperature data used in this study can be found in this series. Computation of the anomaly fields was similar to our earlier work (*7*), but some procedures were changed (*7*).

To estimate changes in heat content at depths greater than 300 m, we prepared objective analyses of running 5-year composites of all historical oceanographic observations of temperature for the period 1948 to 1996 at standard depth levels from the surface through 3000-m depth using the procedures described above. Constructing composites of deep-ocean data by multiyear periods is necessary due to the lack of deep-ocean observations. Most of the data from the deep ocean are from research expeditions. The amount of data at intermediate and deep depths decreases as we go back further in time.

Temporal Variability of Upper Ocean Heat Content

Figure 1 shows the variability of yearly heat content anomalies in the upper 300 m for 1948 to 1998 for individual ocean basins defined using the Equator as a boundary. Each yearly estimate includes the standard error of the mean anomaly value for each year plotted as a vertical bar. The anomaly fields for the Atlantic and Indian oceans, for both the entire basins and Northern and Southern Hemisphere basins of each ocean, show a positive correlation. In each basin before the mid-1970s, temperatures were nearly all relatively cool, whereas after the mid-1970s these oceans are in a warm state. The year of largest yearly mean temperature and heat content for the North Atlantic is 1998. In 1998 heat content reaches a value of $\sim 4 \times 10^{22}$ J, equivalent to a volume mean temperature anomaly of 0.37°C. [Expanded versions of Figs. 1 and 4 with volume mean temperature scales as well as heat content scale and similar time series for heat content integrated through 1000-m depth can be viewed at *Science* Online (*14*) as Web figures 1 to 3.]

Both Pacific Ocean basins exhibit quasi-bidecadal changes in upper ocean heat content, with the two basins positively correlated. During 1997 the Pacific achieved its maximum heat content. A decadal-scale oscillation in North Pacific sea surface temperature (Pacific Decadal Oscillation) has been identified (*15*, *16*), but it is not clear if the variability we observe in Pacific Ocean heat content is correlated with this phenomenon or whether there are additional phenomena that contribute to the observed heat content variability.

In order to place our results in perspective, we compare the range of upper ocean heat content with the range of the climatological annual cycle of heat content for the Northern Hemisphere and world ocean computed as described by (*8*) but using a more complete oceanographic database (*10–13*). There is relatively little contribution to the climatological range of heat content from depths below 300 m. Our results indicate that the decadal variability of the upper ocean heat content in each basin is a significant percentage of the range of the annual cycle for each basin. For example, the climatological range of heat content for the North Atlantic is about 5.6×10^{22} J, and the interdecadal range of heat content is about 3.8×10^{22} J.

Changes in Temperature at 1750-m Depth in the North Atlantic Ocean

Figure 2, A and B, shows the changes of temperature at a depth of 1750 m for 1970–74 minus 1955–59 (Fig. 2A) and for 1988–92 minus 1970–74 (Fig. 2B). The difference field for the two earlier periods shows that much of the North Atlantic was warming between these periods, with the exception of a region of cooling associated with the Mediterranean Outflow (*17*, *18*). The difference field between the later two pentads demonstrates the opposite picture. The subarctic has cooled, with the magnitude of maximum changes exceeding 0.4°C in the Labrador Sea. Parts of the midlatitudes and subtropical

National Oceanographic Data Center/National Oceanic and Atmospheric Association (NODC/NOAA), E/OC5, 1315 East West Highway, Silver Spring, MD, 20910, USA.

*To whom correspondence should be addressed. E-mail: slevitus@nodc.noaa.gov

regions have also cooled substantially. Maximum warming is associated with the tongue of temperature associated with the Mediterranean Outflow. The changes in salinity at this depth (not shown) in both sets of pentadal differences are positively correlated with the changes in temperature, with the result that these changes in temperature and salinity are at least partially density compensating. Tests of statistical significance (Student's *t* test) have been performed on these difference fields, and we find (not shown) that the changes over most of the North Atlantic are statistically significant, as was found for the earlier pentadal differences (*18*). The observed changes are not small and can make an appreciable contribution to Earth's heat balance on decadal time scales, which we quantify in the next section.

Heat Storage of the North Atlantic

Figure 3, A and B, shows the heat storage (computed as the time derivative of heat content) for the 0 to 300 m (Fig. 3A) and 0 to 3000 m (Fig. 3B) layers of the North Atlantic between the 1970–74 and 1988–92 pentads (using the midpoints of the two pentads to compute the time difference between periods). This figure clearly indicates that maximum heat storage for this basin occurs at depths exceeding 300 m.

Cooling occurred throughout the subarctic gyre, with the maximum heat storage exceeding 6 W m^{-2} in the Labrador Sea. Warming occurred in the midlatitudes and subtropics, with values exceeding 8 W m^{-2} in the midlatitudes of the western North Atlantic. We have computed the contribution to the vertically integrated field shown in Fig. 3B from each 500-m layer of the North Atlantic. The cooling of the Labrador Sea is composed of nearly equal contributions of about 1.0 W m^{-2} from each 500-m-thick ocean layer down to 2500-m depth. The warming in the western midlatitudes is due to nearly equal contributions by the 0- to 500- and 500- to 1000-m layers, with some small contributions from deeper layers. The warming associated with the Mediterranean Outflow is mainly due to contributions from the 1000- to 2000-m layer.

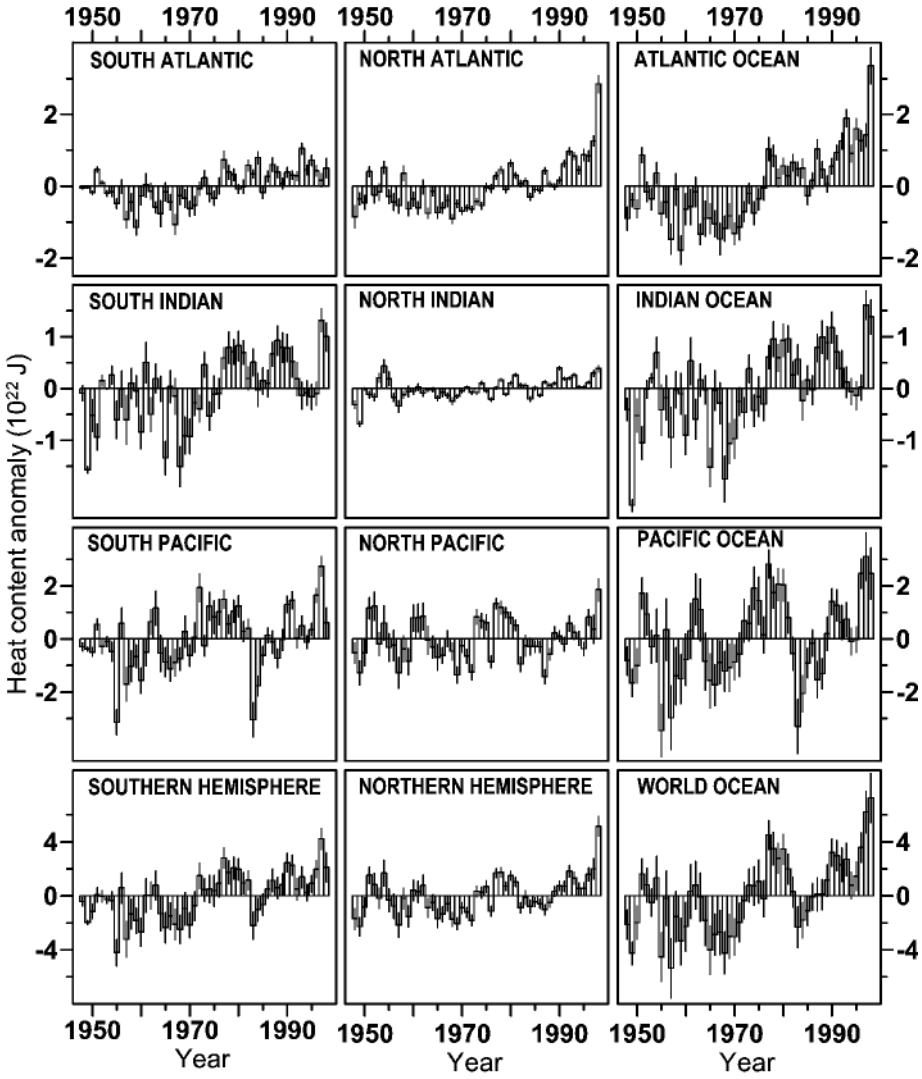

Fig. 1. Time series for the period 1948 to 1998 of ocean heat content (10^{22} J) in the upper 300 m for the Atlantic, Indian, Pacific, and world oceans. Note that 1.5×10^{22} J equals 1 W·year·m^{-2} (averaged over the entire surface of Earth). Vertical lines though each yearly estimate represent ± 1 standard error (SE) of the estimate of heat content. Expanded versions of these figures with equivalent volume mean temperature scales added can be seen at *Science* Online (*14*).

Temporal Variability of Heat Content for the World Ocean

Figure 4 shows the heat content for 5-year running composites by individual basins integrated through 3000-m depth. Only the Atlantic exhibits a substantial contribution to these basin integrals below 1000-m depth. We present the distributions through 3000-m depth for consistency.

There is a consistent warming signal in each ocean basin, although the signals are not monotonic. The signals between the Northern and Southern Hemisphere basins of the Pacific and Indian oceans are positively correlated, suggesting the same basin-scale forcings. The temporal variability of the South Atlantic differs significantly from the North Atlantic, which is due to the deep convective processes that occur in the North Atlantic. Before the 1970s, heat content was generally negative. The Pacific and Atlantic oceans have been warming since the 1950s, and the Indian Ocean has warmed since the 1960s. The delayed warming of the Indian Ocean with respect to the other two oceans may be due to the sparsity of data in the Indian Ocean before 1960. The range of heat content for this series is on the order of 20×10^{22} J for the world ocean.

Discussion

Our results demonstrate that a large part of the world ocean has exhibited coherent changes of ocean heat content during the past 50 years, with the world ocean exhibiting a net warming. These results have implications for climate system research and monitoring efforts in several ways. We cannot partition the observed warming to an anthropogenic component or a component associated with natural variability. Modeling studies are required even to be able to attempt such a partition. However, our results support the findings of Hansen *et al.* (*19*), who concluded that a planetary radiative disequilibrium of about 0.5 to 0.7 W m^{-2} existed for the period 1979 to 1996 (with the Earth system gaining heat) and suggested that the "excess heat must primarily be accumulating in the ocean." Hansen *et al.* included estimates of the radiative forcings from volcanic aerosols, stratospheric ozone depletion, greenhouse gases,

and solar variability. Such information is critical for studies attempting to identify anthropogenic changes in Earth's climate system. This is because coupled air-sea general circulation model experiments that are used to assess the effects of increasing carbon dioxide frequently begin integration with a sudden increase of atmospheric carbon dioxide (e.g., twice the present value) rather than the gradual buildup observed in nature. This is done to minimize computer time required for completion of the time integrations of these numerical experiments. Integration in this manner introduces what is known as a "cold start" error (*20*, *21*).

Global sea surface temperature time series (*1*) for the past 100 years show two distinct warming periods. The first occurred during the period 1920 to 1940 and was followed by a period of cooling; the second warming began during the 1970s. It is important to note that the increase in ocean heat content preceded the observed warming of sea surface temperature. It is not clear what physical mechanisms may be responsible for the observed increase in ocean heat content. The warming could be due to natural variability, anthropogenic effects, or more likely a combination of both. It may seem implausible that subsurface ocean warming preceded the observed global mean warming of surface air and sea surface temperature. This phenomenon is possible because the density of sea water is a function of salinity as well as temperature. Thus, relatively warm and salty water or cold and fresh water can reach subsurface depths from a relatively small region of the sea surface through the processes of convection and/or subduction and can then spread out and warm or freshen a much larger region such as an entire gyre or basin. This is clearly occurring in the North Atlantic Ocean by the mechanism of deep ocean convection (Fig. 2). Lazier (*22*) has documented the cooling and freshening of the deep Labrador Sea that began with the renewal of deep convection in the early 1970s. Dickson *et al.* (*23*) have related the renewal of convection in the Labrador Sea to the North Atlantic Oscillation (NAO) in sea-level pressure.

Nerem *et al.* (*24*) showed for the period 1993 to 1998 that a relative maximum in global mean sea level and sea surface temperature [based on TOPEX/Poseidon altimetric measurements and the Reynolds sea surface temperature analyses (*25*)] occurred at the beginning of 1998. This was associated with the occurrence of El Ñino. Global sea level began decreasing during the rest of 1998. Part of the reason for extreme values in North Atlantic heat content observed during 1998 may be related to the 1997 El Ñino, but additional analyses are required to understand the large increase in the North Atlantic heat content between 1997 and 1998. In addition, we emphasize that the extreme warmth of the world ocean during the mid-1990s was in part due to a multidecadal warming of the Atlantic and Indian oceans as well as a positive polarity in a possible bidecadal oscillation of Pacific Ocean heat content.

One possible link between the Northern Hemisphere oceans and the atmosphere may be found in recent research culminating in the publication by Thompson and Wallace (*26*). Their work indicates that the NAO may in fact be part of a hemispheric mode of sea-level pressure termed the Arctic Oscillation.

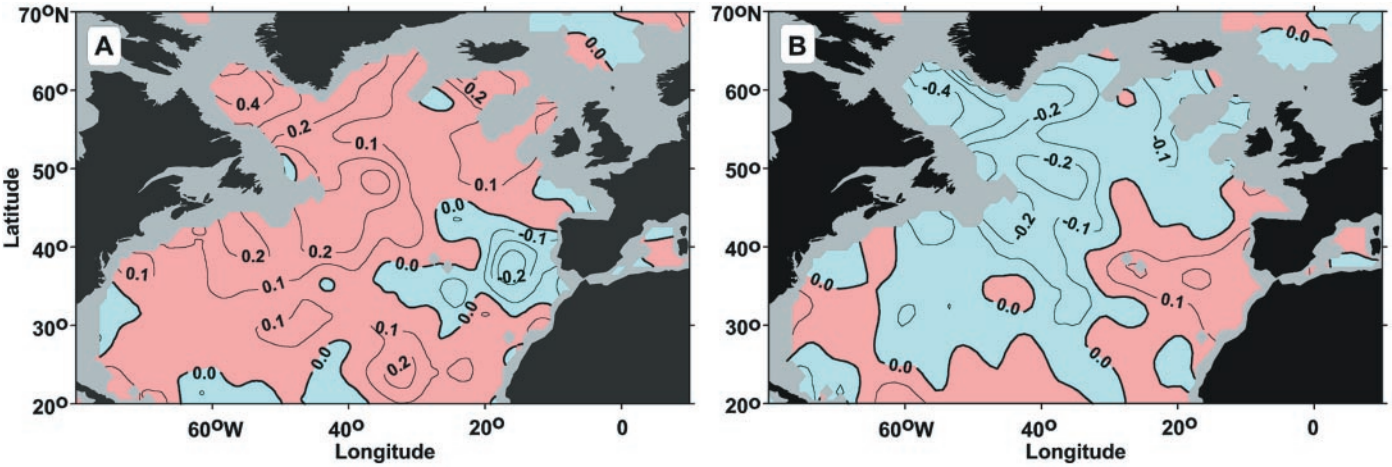

Fig. 2. Temperature difference (°C) at 1750-m depth of the North Atlantic for (**A**) 1970–74 minus 1955–59 and (**B**) 1988–92 minus 1970–74.

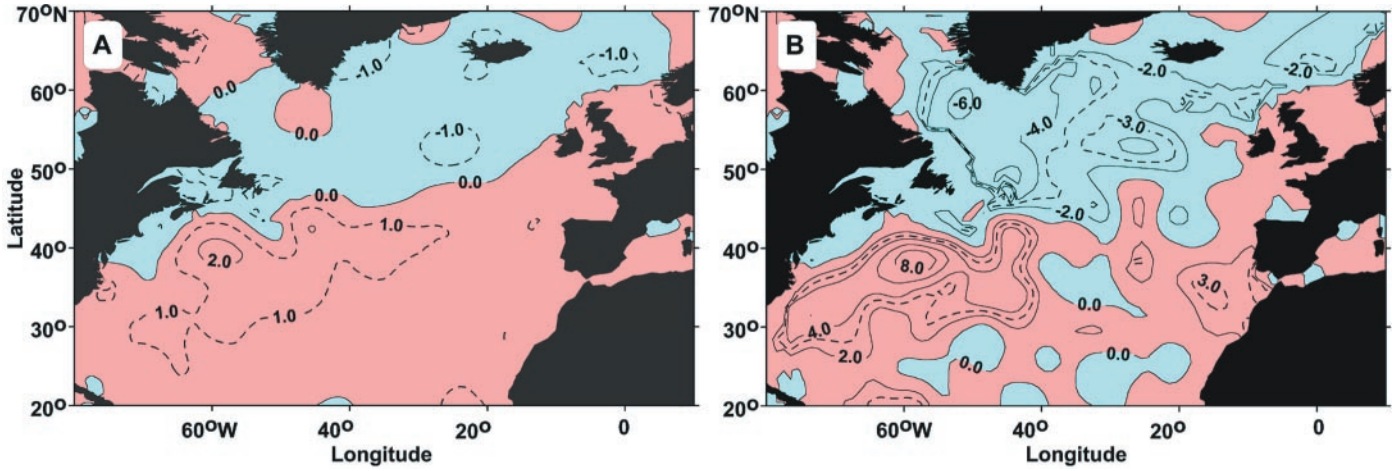

Fig. 3. Heat storage (W m^{-2}) for the North Atlantic for 1988–92 minus 1970–74. (**A**) Integral between the surface and 300-m depth; (**B**) integral between the surface and 3000-m depth.

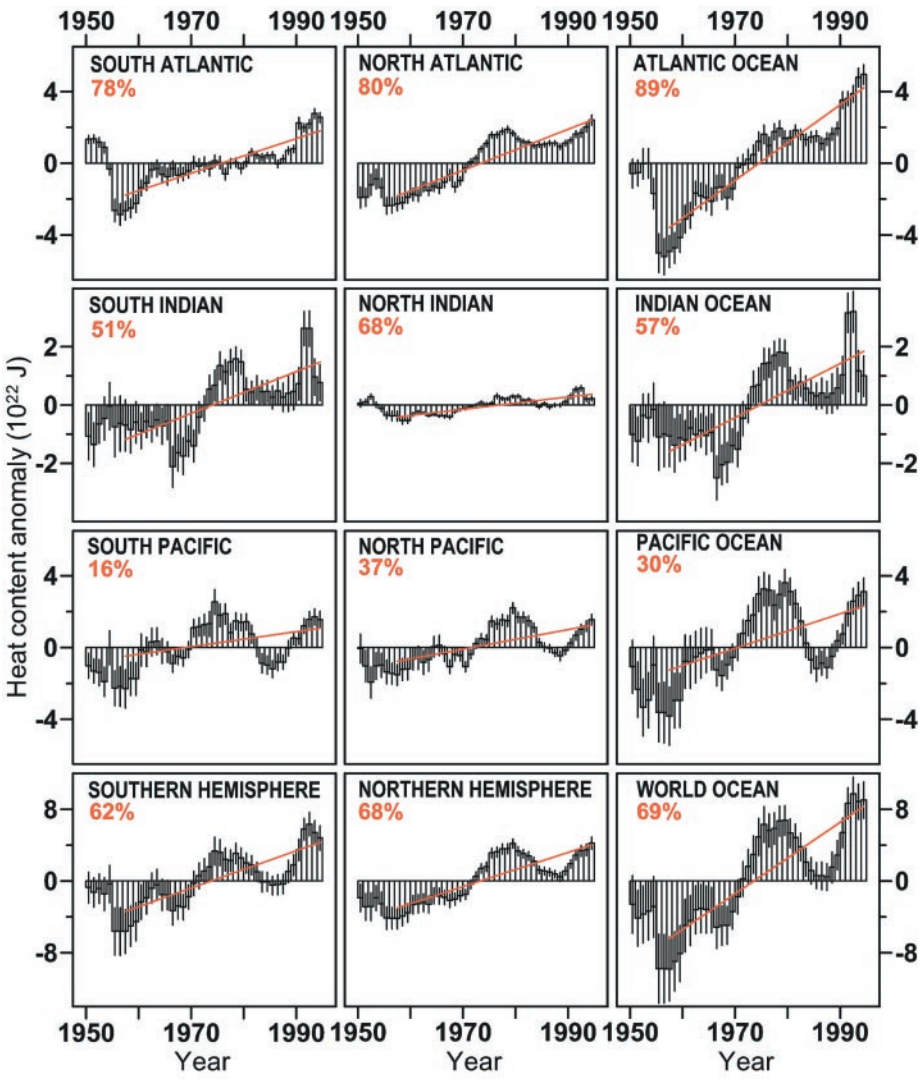

Fig. 4. Time series of 5-year running composites of heat content (10^{22} J) in the upper 3000 m for each major ocean basin. Vertical lines represent ± 1 SE of the 5-year mean estimate of heat content. The linear trend is estimated for each time series for the period 1955 to 1996, which corresponds to the period of best data coverage. The trend is plotted as a red line. The percent variance accounted for by this trend is given in the upper left corner of each panel. Expanded versions of these figures with equivalent volume mean temperature scales added can be viewed at *Science* Online (*14*).

These authors also relate changes at sea level associated with the NAO to changes at the 500-mb height of the atmosphere. Recently, other investigators have related changes in the Northern Hemispheric stratospheric circulation to tropospheric changes related to the NAO pattern (*27*–*31*). Dickson *et al.* (*23*) have correlated convection in the Labrador Sea with the polarity of the NAO. To the extent that these relations are found to be statistically significant, it may be that changes we observe in global ocean heat content may be related to the hemispheric and/or global modal variability of the atmosphere, from sea level through the stratosphere. Determining such possible links is a major part of understanding the mechanisms that govern the state of Earth's climate.

Our final point relates to the large change in Atlantic heat storage from depths exceeding 300 m. Because convection can result in mixing of water through the entire 2000-m depth of the water column in the Labrador Sea, changes in sea surface temperature may remain relatively small in this region despite a large heat flux from ocean to atmosphere. This flux is responsible for the large changes of heat content we have documented at 1750-m depth. This may be an important consideration when comparing the relative role of the tropics and high-latitude convective regions in effecting climate change, whether due to natural or anthropogenic causes.

References and Notes

1. Intergovernmental Program on Climate Change, *Climate Change 1995: The Science of Climate Change, the Contribution of Working Group 1 to the Second Assessment Report of the Intergovernmental Panel on Climate Change* (Cambridge Univ. Press, Cambridge, UK, 1996).
2. CLIVAR, *CLIVAR Science Plan*, World Climate Research Programme, WCRP-89 (WMO/TD NO. 690), 1995.
3. National Research Council, *Global Environmental Change: Research Pathways for the Next Decade* (National Academy Press, Washington, DC, 1999).
4. G. C. Simpson, *Mem. R. Meteorol. Soc.* (1929), p. 53.
5. C. Rossby, in *The Atmosphere and Sea in Motion* (Rockefeller Institute, New York, 1959).
6. J. I. Antonov, *J. Clim.* **6**, 1928 (1993).
7. S. Levitus, T. P. Boyer, J. I. Antonov, *World Ocean Atlas 1994*, vol. 5, *Interannual Variability of Upper Ocean Thermal Structure. NOAA Atlas NESDIS 5* (U.S. Government Printing Office, Washington, DC, 1994). Temperature anomaly values at each standard level in each temperature profile were computed by subtracting the climatological temperature value (*17*) for the month in which the profile was measured. Data values exceeding 3 standard deviations (SDs) from the 5° square in which the data occurred were not used to create the climatology. One notable difference between the procedure used to construct the anomaly fields presented in this study and our earlier work (*7*) is that we used a 6-SD check to flag data as not being usable in this study as compared to the 3-SD check used earlier. This change was made after studies indicated that changes in upper ocean temperature associated with data in the 3- to 6-SD range were real. We computed anomaly fields using all data and compared these results with computed fields on the basis of data that did not include values exceeding 3 SDs. After comparing these two sets of fields, it became clear that large-scale anomaly features were being reduced in amplitude by the 3-SD criterion. Therefore we used a 6-SD criterion to flag data for elimination in our anomaly field computations and manually identified and flagged data that created unrealistic small-scale features (typically bull's-eye patterns with wavelengths less than 500 km). For each year or year-season compositing period, all anomaly values were averaged in each 1° square at each standard depth level from the surface to 1000-m depth. Anomaly fields for each compositing period at each standard depth level were created using a first-guess equal to zero at each grid point. Use of zero as a first-guess rather than persistence or some other procedure minimizes the creation of spurious anomalies. Objective analysis of the 1° square anomaly means was performed with the same analysis procedures as given by (*17*).
8. S. Levitus and J. I. Antonov, *Climatological and Interannual Variability of Temperature, Heat Storage and Rate of Heat Storage in the Upper Ocean. NOAA NESDIS Atlas 16* (U.S. Government Printing Office, Washington, DC, 1997).
9. S. Levitus, R. D. Gelfeld, T. Boyer, D. Johnson, *Results of the NODC and IOC Data Archaeology and Rescue Projects. Key to Oceanographic Records Documentation No. 19* (National Oceanographic Data Center, Washington, DC, 1994).
10. S. Levitus *et al.*, *World Ocean Database 1998*, vol. 1, *Introduction. NOAA Atlas NESDIS 18* (U.S. Government Printing Office, Washington, DC, 1998).
11. T. P. Boyer *et al.*, *World Ocean Database 1998*, vol. 4, *Temporal Distribution of Conductivity-Temperature-Depth Profiles. NOAA Atlas NESDIS 21* (U.S. Government Printing Office, Washington, DC, 1998).
12. T. P. Boyer *et al.*, *World Ocean Database 1998*, vol. 3, *Temporal Distribution of Expendable Bathythermograph Profiles. NOAA Atlas NESDIS 20* (U.S. Government Printing Office, Washington, DC, 1998).
13. T. P. Boyer *et al.*, *World Ocean Database 1998*, vol. 5, *Temporal Distribution of Ocean Station Data (Bottle) Temperature Profiles. NOAA Atlas NESDIS 22* (U.S. Government Printing Office, Washington, DC, 1998).
14. Available at www.sciencemag.org/feature/data/1046907.shl
15. T. Nitta and S. Yamada, *J. Meteorol. Soc. Jpn.* **67**, 375 (1989).
16. K. E. Trenberth, in *Greenhouse-Gas-Induced Climatic Change: A Critical Appraisal of Simulations and Observations*, M. E. Schlesinger, Ed. (Elsevier, Amsterdam, 1991), pp. 377–390.
17. J. I. Antonov *et al.*, *World Ocean Atlas 1998*, vol. 1, *Atlantic Ocean Temperature Fields. NOAA Atlas NESDIS 27* (U.S. Government Printing Office, Washington, DC, 1998). There are similar volumes in this series for the Pacific and Indian oceans.

18. S. Levitus, *J. Geophys. Res. Oceans*, **94**, 6091 (1989).
19. J. Hansen *et al.*, *J. Geophys. Res.* **102**, 25679 (1997).
20. K. Hasselmann, R. Sausen, E. Maier-Reimer, R. Voss, *Clim. Dyn.* **9**, 53 (1993).
21. J. Hansen *et al.*, *J. Geophys. Res.* **93**, 9341 (1988).
22. J. R. N. Lazier, in *Natural Climate Variability on Decade-to-Century Time Scales*, D. G. Martinson *et al.*, Eds. (National Academy Press, Washington, DC, 1995), chap. 3, pp. 295–302.
23. R. Dickson, J. Lazier, J. Meincke, P. Rhines, J. Swift, *Prog. Oceanogr.* **38,** 241 (1996).
24. S. Nerem, D. P. Chambers, E. W. Leuliette, G. T. Mitchum, B. S. Giese, *Geophys. Res. Lett.* **26**, 3005 (1999).
25. R. W. Reynolds and T. S. Smith, *J. Clim.* 7, 929 (1994).
26. D. W. J. Thompson and J. M. Wallace, *Geophys. Res. Lett.* **25**, 1297 (1998).
27. D. T. Shindell *et al.*, *Nature*, **399**, 452 (1999).
28. J. Perlwitz and H.-F. Graf, *J. Clim.* **8**, 2281 (1995).
29. A. Kitoh *et al.*, *Geophys. Res. Lett.* **23**, 543 (1996).
30. M. P. Baldwin *et al.*, *Geophys. Res. Lett.* **21**, 1141 (1994).
31. X. Cheng and T. J. Dunkerton, *J. Clim.* **8**, 2631 (1995).
32. The construction of the analyses shown in this work was supported by grants from the NOAA Climate and Global Change program. Preparation of the databases used in this work was supported by the NOAA and NOAA/NASA Climate and Global Change programs and the NOAA ESDIM program. J.I.A. is a University Corporation for Atmospheric Research (UCAR) Project Scientist at NODC/NOAA.

8 November 1999; accepted 11 February 2000

A *Drosophila* Mechanosensory Transduction Channel

Richard G. Walker,[1] Aarron T. Willingham,[1] Charles S. Zuker[2]*

Mechanosensory transduction underlies a wide range of senses, including proprioception, touch, balance, and hearing. The pivotal element of these senses is a mechanically gated ion channel that transduces sound, pressure, or movement into changes in excitability of specialized sensory cells. Despite the prevalence of mechanosensory systems, little is known about the molecular nature of the transduction channels. To identify such a channel, we analyzed *Drosophila melanogaster* mechanoreceptive mutants for defects in mechanosensory physiology. Loss-of-function mutations in the *no mechanoreceptor potential C* (*nompC*) gene virtually abolished mechanosensory signaling. *nompC* encodes a new ion channel that is essential for mechanosensory transduction. As expected for a transduction channel, *D. melanogaster* NOMPC and a *Caenorhabditis elegans* homolog were selectively expressed in mechanosensory organs.

Our capacity to hear a whisper across a crowded room, detect our position in space, and coordinate our limbs during a stroll through the park is conferred by the mechanical senses. Mechanosensory transduction is the process that converts mechanical forces into electrical signals. When mechanoreceptors are stimulated, mechanically sensitive cation channels open and produce an inward transduction current that depolarizes the cell. The opening of mechanosensory transduction channels in vertebrate hair cells takes place within a few microseconds after the onset of a stimulus, too quickly for the generation of second messengers (*1*). Mechanical stimuli are therefore hypothesized to directly gate these channels. This mode of activation is in sharp contrast to other sensory modalities, such as vision, olfaction, and taste, which use stereotypical G protein–coupled cascades to modulate transduction channels.

Most models of mechanosensory signaling propose that transduction channels be anchored on both sides of the membrane, so that relative movements between the extracellular matrix and the cytoskeleton produce the mechanical tension that gates these channels. In the gating-spring model of mechanosensory transduction in vertebrate hair cells (*2, 3*), deflection of the mechanically sensitive hair bundle produces shear between adjacent stereocilia that stretches the gating springs. This increase in tension "pulls" the transduction channels open, depolarizes the cell, and triggers neurotransmitter release. Although biophysical data support this model for transduction in hair cells, the molecular identity of the mechanically gated ion channel remains unknown. This is largely due to the paucity of sensory tissue and the small number of transduction channels in each hair cell (*4*).

Genetic approaches are ideally suited for identifying rare molecules involved in mechanosensory transduction (*5–10*). The isolation of genetic mutations does not depend on any assumptions about the nature or abundance of the target molecules, other than loss of their function results in a recognizable phenotype. The most extensive genetic dissection of mechanosensory behavior was based on screens for *Caenorhabditis elegans* touch-insensitive mutants. These studies identified genes involved in the development, survival, function, and regulation of touch receptor neurons (*11*). Of particular interest were those that likely function in the mechanoelectrical transduction process. This group included degenerins, collagen, stomatin, and tubulins, a finding consistent with the expectation that mechanosensory signaling involves finely orchestrated interactions between ion channels, extracellular matrix, and cytoskeletal components (*12*).

Degenerins (MEC-4, MEC-10, DEG-1, UNC-8, and UNC-105) are a family of *C. elegans* ion channels related to vertebrate epithelial sodium channels (*13*). Because of their critical role in the touch receptor neurons, degenerins have been proposed to function as mechanosensory transduction channels (*13*). More recently, a *C. elegans* transient receptor potential (TRP) family member, OSM-9, was shown to be involved in mechanotransduction because it is expressed in sensory dendrites of a subset of ciliated sensory neurons and is required for osmosensation and nose touch (*14*). Although these genetic studies demonstrated the requirement for degenerins and OSM-9 in mechanoreception, there are no electrophysiological data supporting a role for these channels in the actual transduction process.

Drosophila is an attractive model to dissect mechanosensation because it is possible to combine genetic manipulations with electrophysiological recordings from mechanoreceptor neurons (*7*). The fly's mechanosensory repertoire includes touch, proprioception, and hearing, mediated by the complement of sensory bristles, campaniform sensilla, chordotonal organs, and type II mechanoreceptors (*15*). Of these, sensory bristles are particularly amenable to physiological manipulation in the intact animal. Each mechanosensory bristle organ is composed of a hollow hair shaft whose base impinges on the dendritic tip of a bipolar sensory neuron (Fig. 1A). The shaft thus acts as a tiny lever arm in which deflections of the external bristle compress the neuron's dendritic tip and gate the transduction channels (*16*). The mechanosensory dendrite is bathed in an unusual high-K^+, low-Ca^{2+} fluid (*17*), which provides a large positive driving force into the neuron; opening of transduction channels depolarizes the cell and promotes neurotransmitter release.

To identify components of the mechanotransduction machinery, we screened *Drosophila* touch-insensitive and proprioceptive mutants (*7*) for defects in the physiology of mechanosensory responses. Those mutants that most likely defined transduction molecules were then characterized.

Wild-type mechanosensory response. To gain electrical access to the sensory neuron,

[1]Departments of Biology and Neurosciences and [2]Howard Hughes Medical Institute, University of California, San Diego, La Jolla, CA 92093–0649, USA.

*To whom correspondence should be addressed. E-mail: charles@flyeye.ucsd.edu